Radio Signatures from Conversion of axion-like particle to photons

1. ALP-photon conversion in structured magnetic fields
2. Application to Astrophysical Sources
3. Parametric Resonance Conversion of supercritical ALP stars in the Milky Way
4. Conclusions and Outlook

Günter Sigl
II. Institut theoretische Physik, Universität Hamburg

ALP-photon Coupling

fundamental coupling:

$$\frac{\alpha_{\rm em}}{8\pi}\frac{C_{a\gamma}}{f_a}\,a\,F_{\mu\nu}\tilde{F}^{\mu\nu} = \frac{e^2}{32\pi^2}\frac{C_{a\gamma}}{f_a}\,a\,F_{\mu\nu}\tilde{F}^{\mu\nu} = \frac{\alpha_{\rm em}}{8\pi}\frac{C_{a\gamma}}{f_a}\,a\,F_{\mu\nu}\tilde{F}^{\mu\nu} = \frac{g_{a\gamma}}{4}\,a\,F_{\mu\nu}\tilde{F}^{\mu\nu}\,, \tag{4}$$

where $\alpha_{\rm em} = e^2/(4\pi\epsilon_0)$ and

$$g_{a\gamma} \equiv \frac{\alpha_{\rm em} C_{a\gamma}}{2\pi f_a}\,. \tag{5}$$

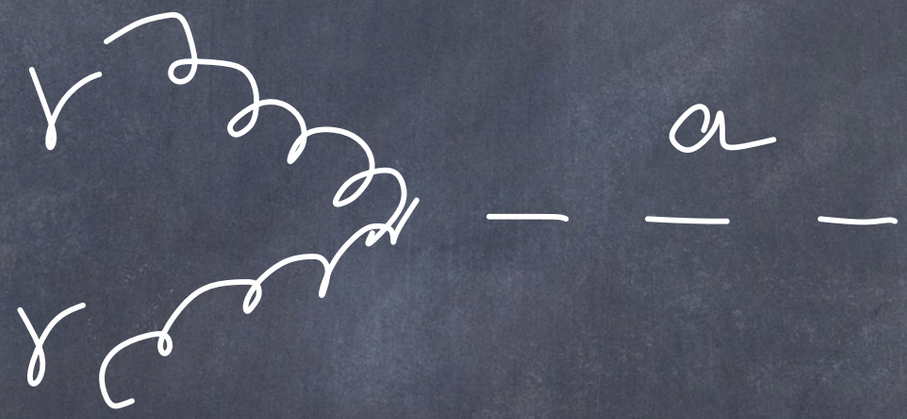

can give rise to following effects:

- Primakoff conversions between ALPs and photons in background electromagnetic fields -> shining light through a wall, helioscopes, haloscopes
- modified photon refraction in ALP background -> Mathieu-type equations
- parametric amplification of photon amplitudes in ALP background -> Mathieu-type equations

Current Constraints and Future Sensitivities

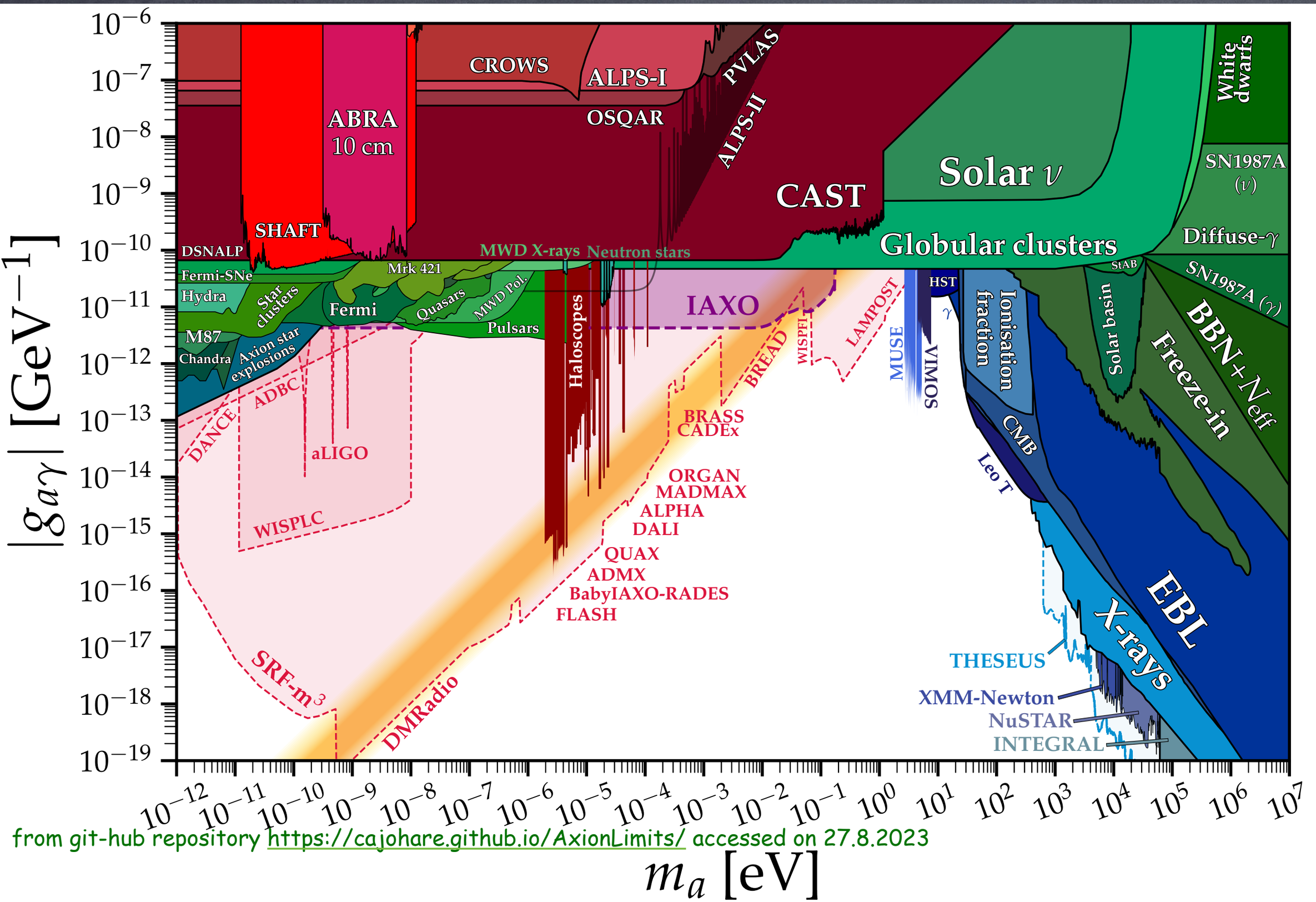

from git-hub repository https://cajohare.github.io/AxionLimits/ accessed on 27.8.2023

ALP-photon Conversion in Structured Magnetic Fields

The following is based on GS, Phys.Rev. D96 (2017) 103014 [arXiv:1708.08908]

Energy-momentum conservation: quantities for ALP, photon and magnetic field carry subscript a, γ, or none, respectively:

$$E_a = (m_a^2 + \mathbf{k}_a^2)^{1/2} = \omega_\gamma - \omega = (\omega_{\rm pl}^2 + \mathbf{k}_\gamma^2)^{1/2} - \omega\,, \quad \mathbf{k}_a = \mathbf{k}_\gamma - \mathbf{k}\,,$$

where the plasma frequency is given by:

$$\omega_{\rm pl} = \left(\frac{e^2 n_e}{\epsilon_0 m_e}\right)^{1/2} \simeq 5.6 \times 10^4 \left(\frac{n_e}{\rm cm^{-3}}\right)^{1/2} \,{\rm rad\,s^{-1}}\,.$$

propagation of converted photons requires $m_a \gg \omega_{pl}$. This will be the case for the objects considered here.

Also assume n_e ~ constant here (non-resonant conversion)

recently K. Kelley and P. J. Quinn, Astrophys. J. 845, 1 (2017) [arXiv:1708.01399] pointed out the possibility to search for ALP dark matter with radio telescopes; they used standard magnetic field estimates but assumed most of the power is on meter scales which is unlikely.

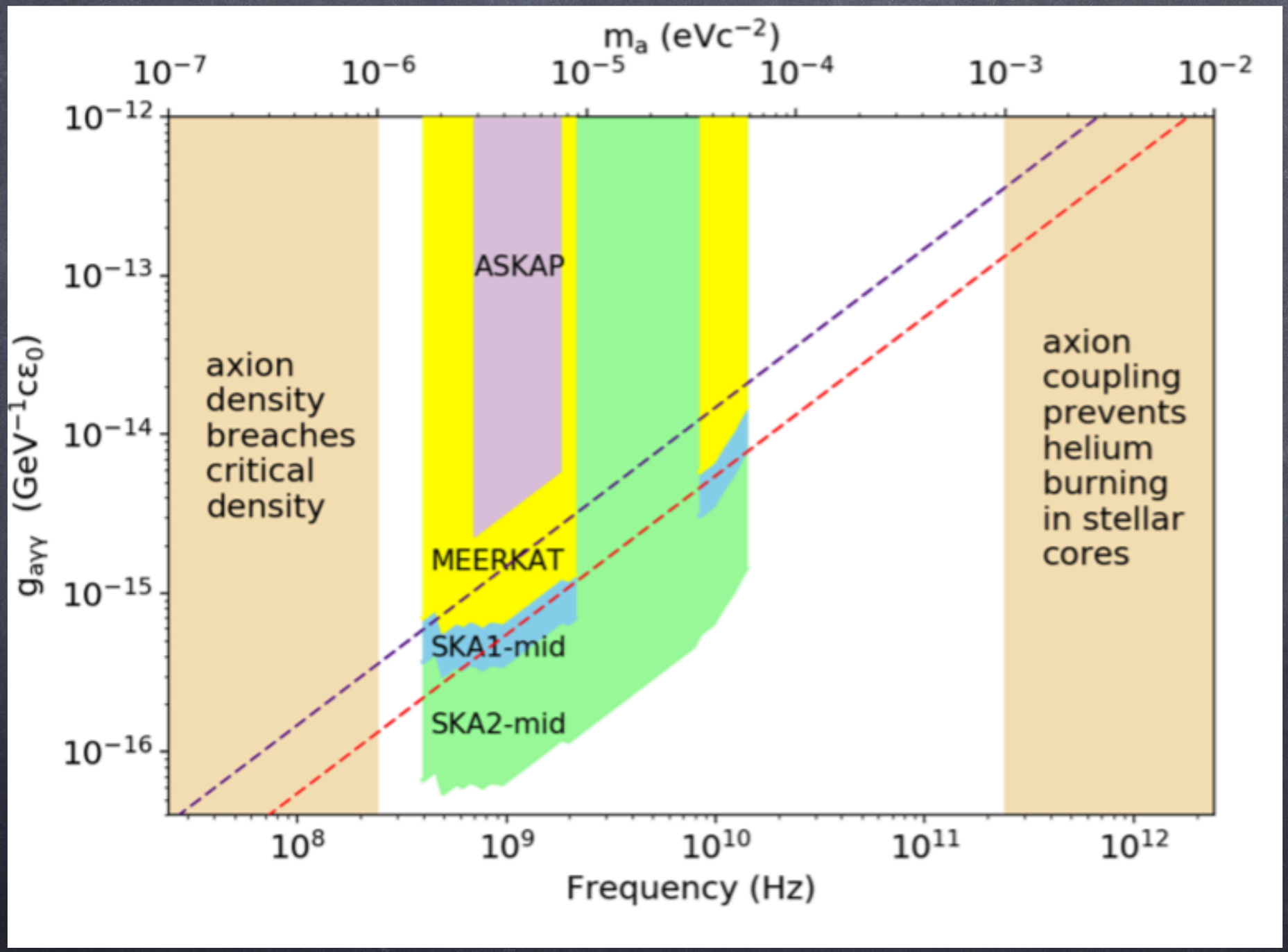

For a source at distance d containing total ALP mass M_a one similarly gets the **total flux density (Jansky)**

$$S \simeq \frac{\pi}{4d^2}\frac{g_{a\gamma}^2}{m_a^2}\frac{1}{\Delta}\int d^3\mathbf{r}\rho_a(\mathbf{r})\rho_m(m_a,\mathbf{r}) \simeq \frac{\pi}{4d^2}\frac{g_{a\gamma}^2}{m_a^2}\frac{1}{\Delta}M_a\rho_m(m_a)\,,$$

For a source radius r_s this corresponds to the **specific intensity** $I=S/\Omega_s$, which is independent of the distance:

$$I \simeq \frac{1}{4r_s^2}\frac{g_{a\gamma}^2}{m_a^2}\frac{1}{\Delta}M_a\rho_m(m_a)\,,$$

trade-off: significant small-scale magnetic field power favours small systems (stellar size) but small objects contain few ALPs -> most suitable objects ?

Resonant Primakoff Conversion

Full conversion (e.g. resonance between ALP mass and plasma frequency at distance r_s from neutron star center) gives a maximal flux given by

$$S_{\rm max} \simeq \frac{\rho_a}{m_a}\frac{v_a}{\Delta}\left(\frac{r_s}{d}\right)^2 \simeq 10^{-10}\left(\frac{m_a}{\mu{\rm eV}}\right)^{-1}\left(\frac{r_s}{10^6\,{\rm cm}}\right)^2\left(\frac{d}{\rm kpc}\right)^{-2}{\rm Jy}\,,$$

see also M.S.Pshirkov, J.Exp.Theor.Phys. 108 (2009) 384 [arXiv:0711.1264] who obtained higher fluxes, see also A. Hook et al., Phys.Rev.Lett 121 (2018) 241102 [arXiv:1804.03145], F.P. Huang et al., arXiv:1803.08230

Gravitational effects may increase the flux by factor $\simeq 1/v_a^2$ to $1/v_a^3$. This would be detectable out to galactic distances.

A. Hook et al., Phys.Rev.Lett 121 (2018) 241102 [arXiv:1804.03145] made a more detailed calculation of resonant conversion (when plasma frequency matches ALP mass) around neutron stars which results in

$$\frac{d\mathcal{P}(\theta=\frac{\pi}{2},\theta_m=0)}{d\Omega} \approx 4.5\times10^{8}\ \mathrm{W}\left(\frac{g_{a\gamma\gamma}}{10^{-12}\ \mathrm{GeV}^{-1}}\right)^2 \left(\frac{r_0}{10\ \mathrm{km}}\right)^2\left(\frac{m_a}{1\ \mathrm{GHz}}\right)^{5/3}\left(\frac{B_0}{10^{14}\ \mathrm{G}}\right)^{2/3}\left(\frac{P}{1\ \mathrm{sec}}\right)^{4/3} \left(\frac{\rho_\infty}{0.3\ \mathrm{GeV/cm}^3}\right)\left(\frac{M_{\mathrm{NS}}}{1\ M_\odot}\right)\left(\frac{200\ \mathrm{km/s}}{v_0}\right),$$

$$S = 6.7\times10^{-5}\ \mathrm{Jy}\left(\frac{100\ \mathrm{pc}}{d}\right)^2\left(\frac{1\ \mathrm{GHz}}{m_a}\right)\times \left(\frac{200\ \mathrm{km/s}}{v_0}\right)^2\left[\frac{d\mathcal{P}/d\Omega}{4.5\times10^{8}\ \mathrm{W}}\right].$$

Advantage: Depends on plasma and magnetic field structure only through adiabaticity of conversion (plasma scale height, mixing through magnetic field at resonance)

Line width from one source is order v_a^2 (ALP energy spread, energy conservation, all coming from one direction), whereas order v_a from ensemble of sources (Doppler effect)

A. Hook et al., Phys.Rev.Lett 121 (2018) 241102 [arXiv:1804.03145]

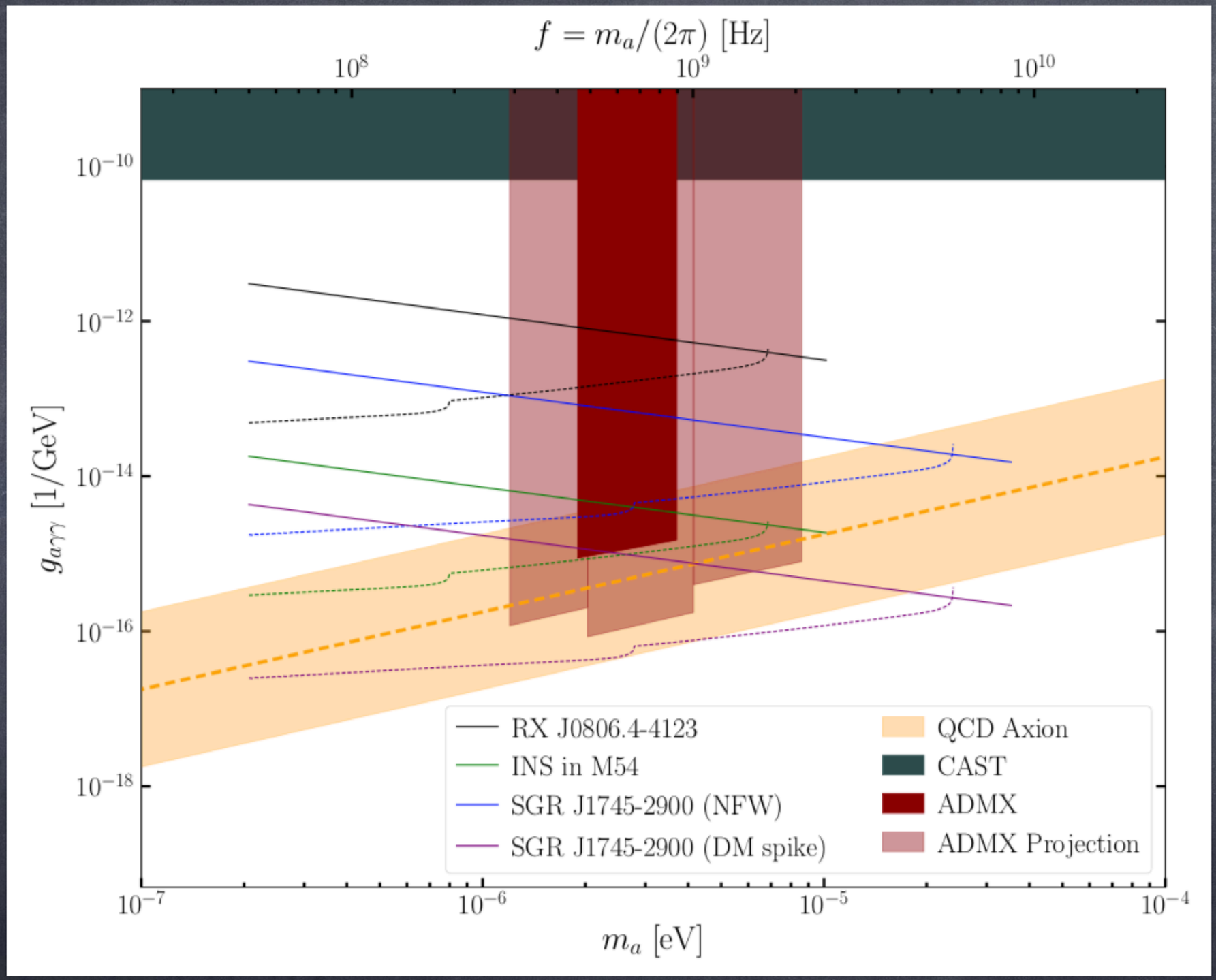

takes into account ALP density enhancement around galactic center (but spike may not be realistic)

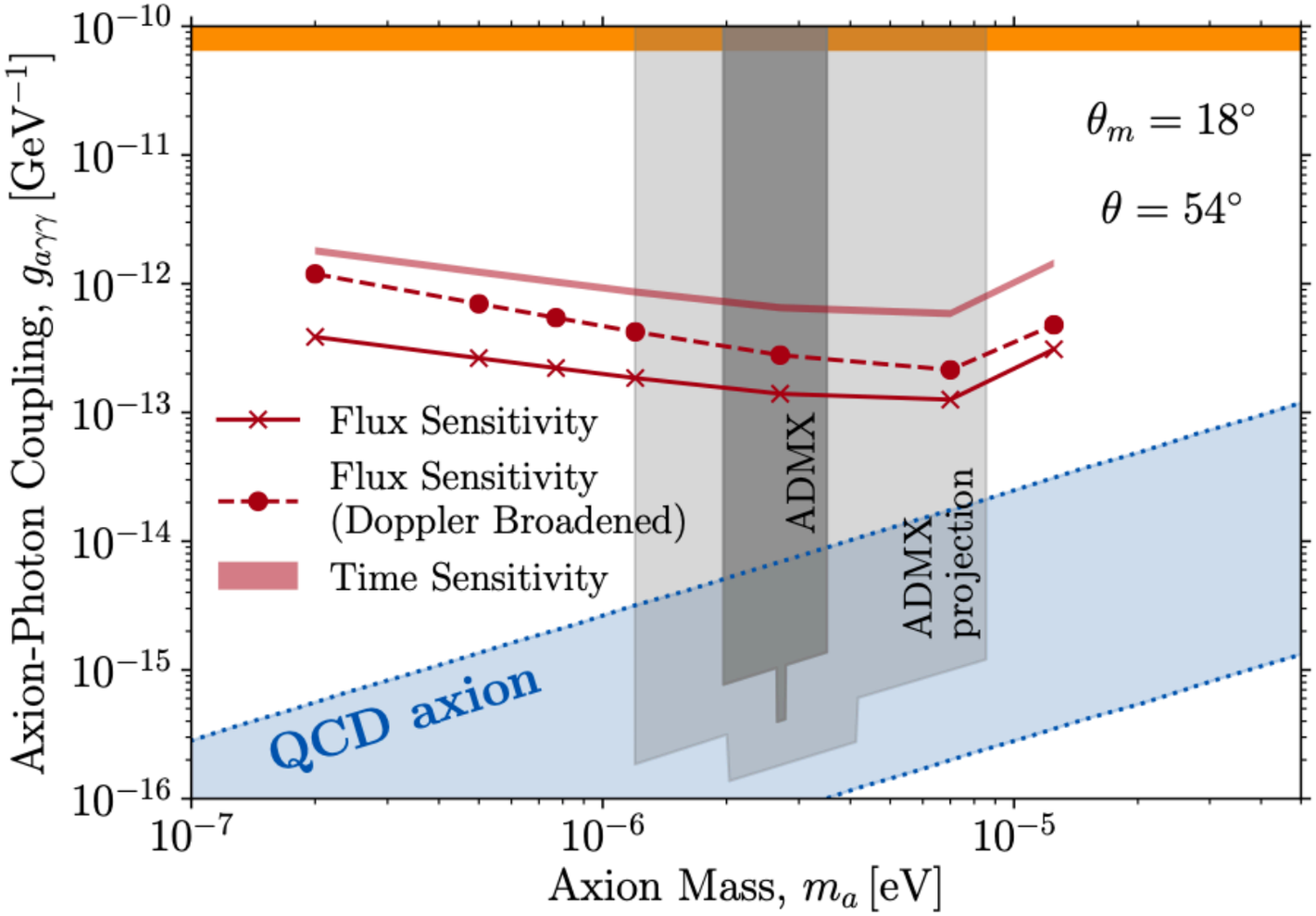

M. Leroy et al., arXiv:1912.08815

FIG. 6. **Projected sensitivity to the axion-photon coupling from radio observations.** We consider the isolated NS J0806.4-412 and assume $\tau_{\rm obs} = 100\,$hrs. The two red lines correspond to the sensitivity limit for two line broadening scenarios as described in the text. The red solid line only accounts for the DM velocity distribution far from the NS where as the red dashed line also accounts for Doppler broadening from the rotation of the NS magnetosphere. The red band shows the minimum coupling required to detect the time variation of the signal (here we neglect Doppler broadening).

resonant axion-photon conversion from ray tracing simulations: line width depends on (complicated) source details

Many more recent works:
R.A. Battye et al, arXiv:2104.08290, arXiv:2107.01225

S.J. Witte et al., arXiv:2104.07670

A.J. Millar et al, arXiv:2107.07399

Recent proposal to consider cumulative fluxes

e.g. from all neutron stars and magnetic white dwarfs in globular clusters such as Omega Centauri, Wang, Bi, Yin, arXiv:2109.00877

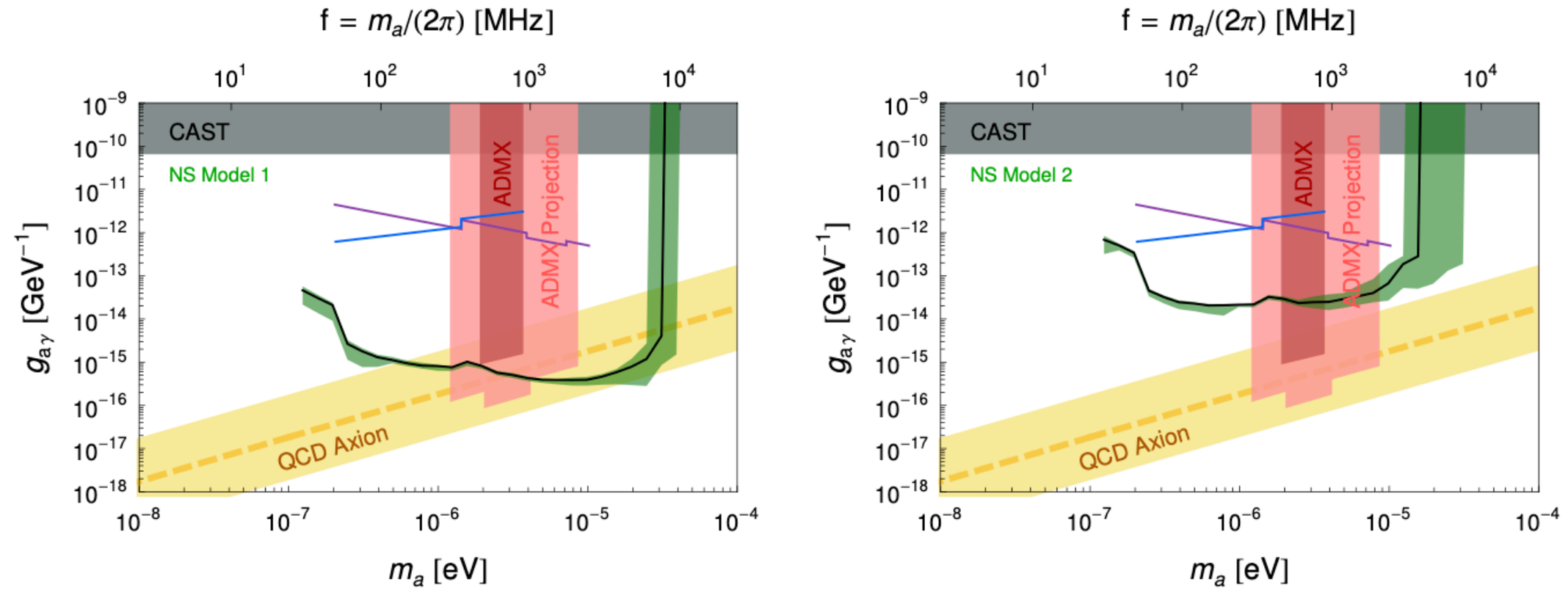

FIG. 6. *The combined projected sensitivity (pure NSs case) to $g_{a\gamma}$ as a function of the axion mass m_a for SKA1 and LOFAR with 100 hours observations of the ω Cen is shown in the green band. The green band contains ten separate sets of NS samples, and its upper and lower boundaries represent the maximum and minimum values, and the black solid line represent the median value. The left panel assumes NS model 1, wile the right panel takes NS model 2. For comparison, the results of the isolated NS RX J0806.4-4123 and MWD WD 2010+310 are shown with purple and blue solid lines. The QCD axion is predicted to lie within the yellow band. The limits set by CAST and ADMX (current and projected) are indicated by the gray and red regions, respectively.*

ALP-Photon Conversion through Parametric Resonance

Tkachev Sov.Astron.Lett. 12 (1986) 305, Pisma Astron.Zh. 12 (1986) 726,
see also M.P. Hertzberg and E.D. Schiappacasse, JCAP 1811 (2018) 004 [arXiv:1805.00430]

From the modified Maxwell equations for a homogeneous ALP field $a(t)=a_0 \sin m_a t$ for a photon momentum mode k one obtains a Mathieu-type equation of the form

$$\left[\frac{d^2}{dx^2} + A - 2q\cos(2x)\right] A_{\pm} = 0$$

for the two circularly polarised photon fields $A_{\pm}$ with $x=m_a t/2$ and

$$A = \frac{4k^2}{m_a^2}, \quad q = \pm \frac{2k}{\epsilon_0 M_a} \frac{a_0}{m_a}$$

For q<1 (narrow resonance) there are resonances at $A = 1 \pm q$ growing with a rate in x of ~ q/2. The resulting band width is $k = m_a(1 \pm q)/2$
This corresponds to the crossed spontaneous decay into $k=m_a/2$ photons.
For q>1 other resonances are at A~2q growing with a rate in x of ~1 (probably not relevant here)

Carenza, Mirizzi, GS, PRD 101 (2020) 103016 [arXiv:1911.07838] performed a more detailed calculation of axion condensate decay into photons:

Number of produced photons in mode **k**:

$$N_{\mathbf{k}}(t) = N_{\mathbf{k}}(0)e^{2\mu t} + 2(\cosh(2\mu t) - 1)$$

Number of converted axions depends on number of photon modes:

$$\Delta N_a \sim N_d N_t [N_{m_a/2}(T) - N_{m_a/2}(0)]$$

where in a clump of size L, $N_d \simeq (Lm_a)^2/(4\pi)$ and $N_t \simeq \mu L/\pi$, see also R.F. Sawyer, arXiv:809.01183 and arXiv:1908.04298. To avoid overproduction of radio background one requires

$$\frac{\Delta N_a}{N_a} f_{\rm dm} \lesssim \frac{\Omega_\gamma(m_a/2)}{\Omega_{\rm dm}} \frac{\Delta\nu}{\nu}$$

which, if dark matter clumps on characteristic scales L, requires

$$\mu L \lesssim \frac{1}{2} \ln \left[\frac{\Omega_\gamma(m_a/2)}{f_{\rm dm}\Omega_{\rm dm}} \frac{N_a}{N_d N_t (N_{m_a/2}(0)+1)} \frac{\Delta\nu}{\nu} \right] \lesssim 30\,.$$

For example, for the axion clumps discussed in Schiappacasse and Hertzberg, Astropart. Phys. 01 (2018) 037; 03 (2018) E01 one has

$$\mu = \frac{1}{\sqrt{8}} g_{a\gamma} \rho_{\rm max}^{1/2} = 1.7 \times 10^{-9} \left(\frac{m_a}{10^{-5}\,{\rm eV}} \right) \left(\frac{g_{a\gamma}}{10^{-11}\,{\rm GeV}^{-1}} \right)^{-1} {\rm km}^{-1}$$

Study of solutions of modified wave equation under study by several groups, see e.g. L. Chen and T.Kephart, arXiv:2002.07885 (Photon directional profile from stimulated decay of axion clouds with arbitrary momentum distributions) and Z. Wang et al., arXiv:2002.09144 (Resonant instability of axionic dark matter clumps)

Parametric Resonance Conversion of supercritical ALP stars in the Milky Way

preliminary work based on Maseizik, Seong, Mondal, Sigl

How do ALP stars accrete ?

1.) optimistic case: growth on gravitational condensation timescale on mini cluster background ("attractor model") based on Levkov et al., PRL 123 (2018) 151301 (see also Levkov et al. PRD 102 (2020) 023501)

Remembering that $\delta M_\star/\delta t \propto M_h/\tau_{gr}$ in eq. 23 with

$$\tau_{gr} \simeq \frac{10^9 \mathrm{yr}}{\Phi^3(1+\Phi)} \left(\frac{M_c}{10^{-13} M_\odot}\right)^2 \left(\frac{m}{26\mu\mathrm{eV}}\right)^3 , \tag{26}$$

and writing the flux obtained from the radio emission of an average axion star as

$$F_\star(\Phi) = \frac{c^2}{4\pi d^2} \frac{\delta M_\star(\Phi, M_h)}{\delta t} , \tag{27}$$

it is clear to see that the observed signal

$$F_{\star,\mathrm{tot}}(\Phi) \propto N_{\star,\gamma}(\Phi) \frac{\delta M_\star}{\delta t} \propto N_{\star,\gamma} p(\Phi) \frac{M_h}{\tau_{gr}} \propto \Phi^3(1+\Phi) \frac{p(\Phi)}{M_h} \tag{28}$$

2.) assume core-halo relation and accretion onto the halo (mini cluster)

$$\frac{\delta M_*(R)}{\delta t} = \frac{1}{3}\left(\frac{M_h}{M_{0,min}}\right)^{-\frac{2}{3}} \frac{\delta M_h(R)}{\delta t} = \frac{4\pi}{3}\left(\frac{M_h}{M_{0,min}}\right)^{-\frac{2}{3}} R_h^2 \rho_{NFW}(R) \langle v(R)\rangle_{\text{eff}}$$

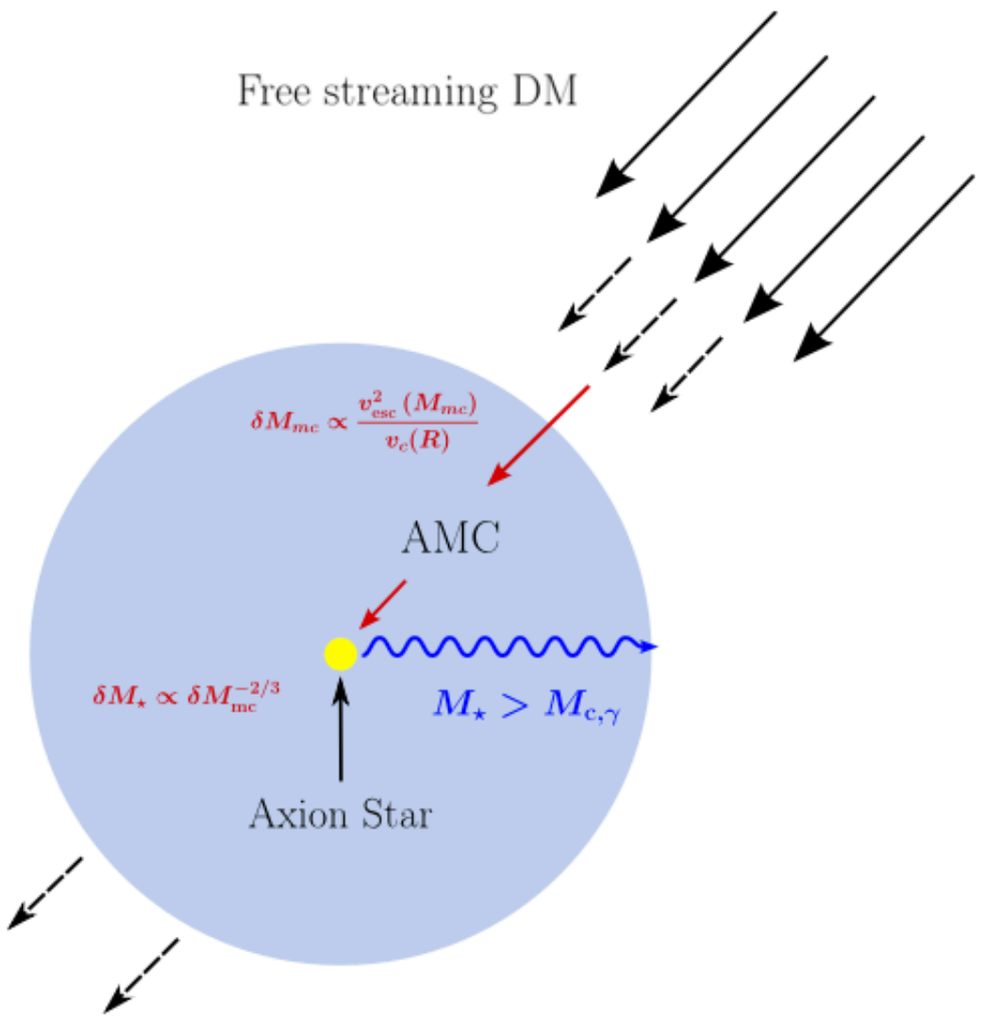

Figure 1: Accretion Model for the Core-halo system capturing gravitationally unbound dark matter from the NFW background of the milky way halo in two stages: First by gravitational capturing onto the minicluster and, secondly, by accretion onto the virializing axion star.

compare with extreme case $\delta M_* = \delta M_h$

one has to integrate over all mini clusters in the Milky Way, assuming that ~ 70% of dark matter is in form of mini clusters, by folding over the mini cluster over density distribution, and integrating over the ALP-photon coupling dependent supercritical ALP star masses

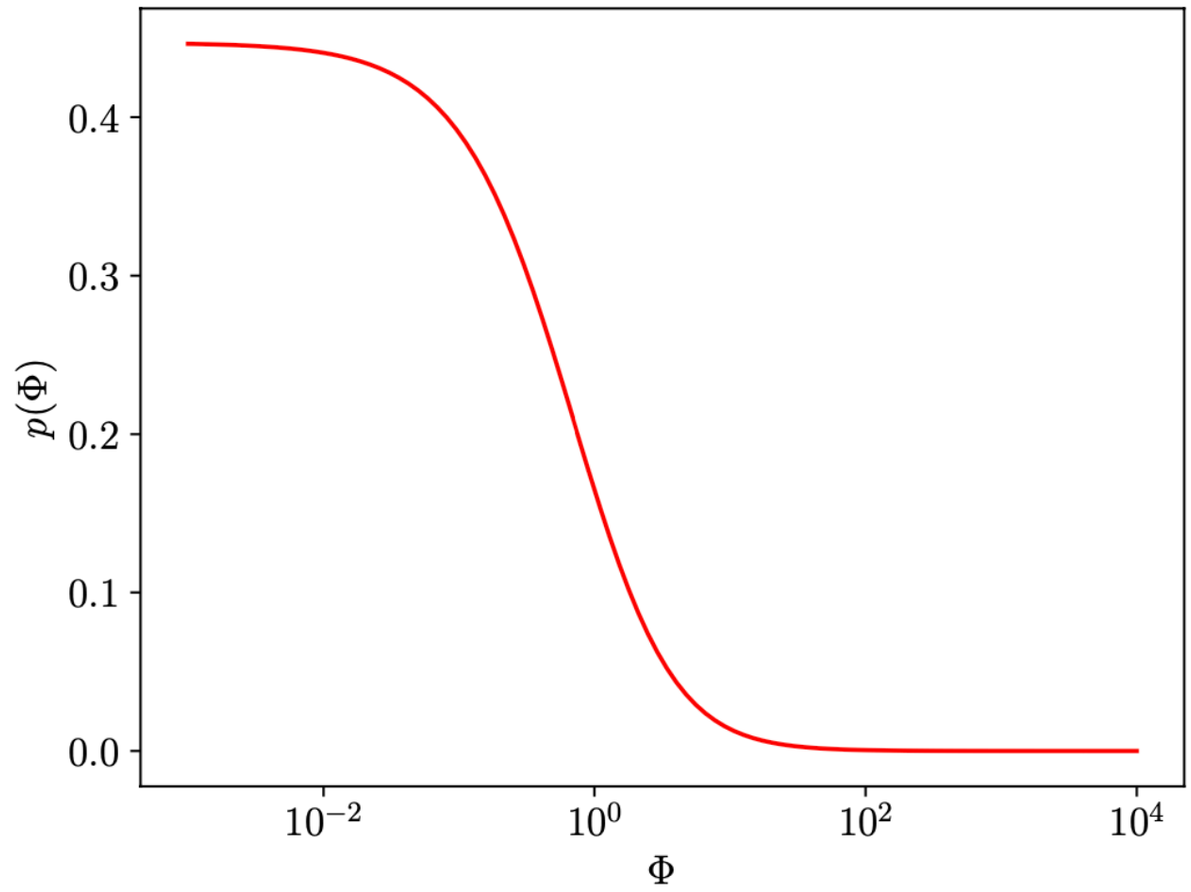

based on Kolb and Tkachev, PRD 50 (1994) 769

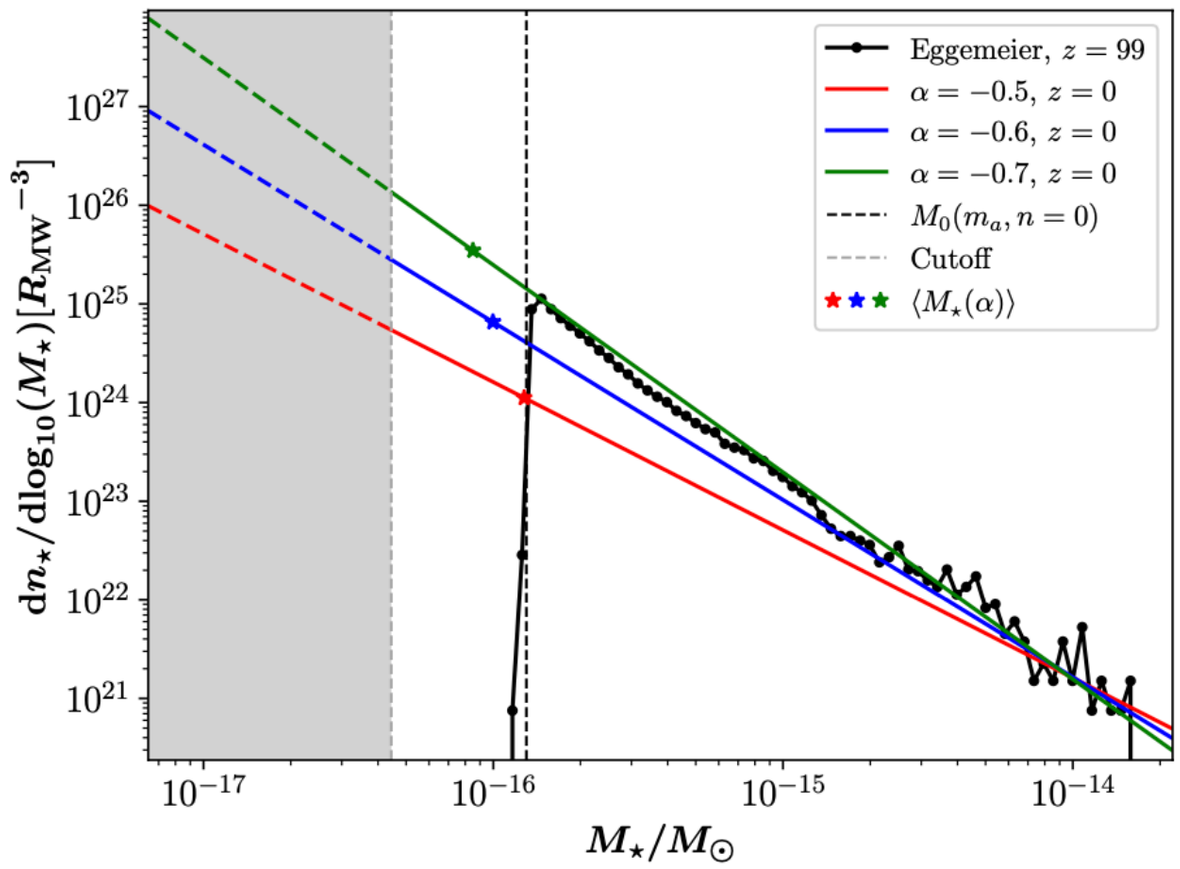

based on Eggemeier et al., PRL 125 (2020) 041301 and Fairbairn at al., PRD 97 (2018) 083502

gravitational condensation accretion rate versus core-halo relation/minicluster growth related accretion rate

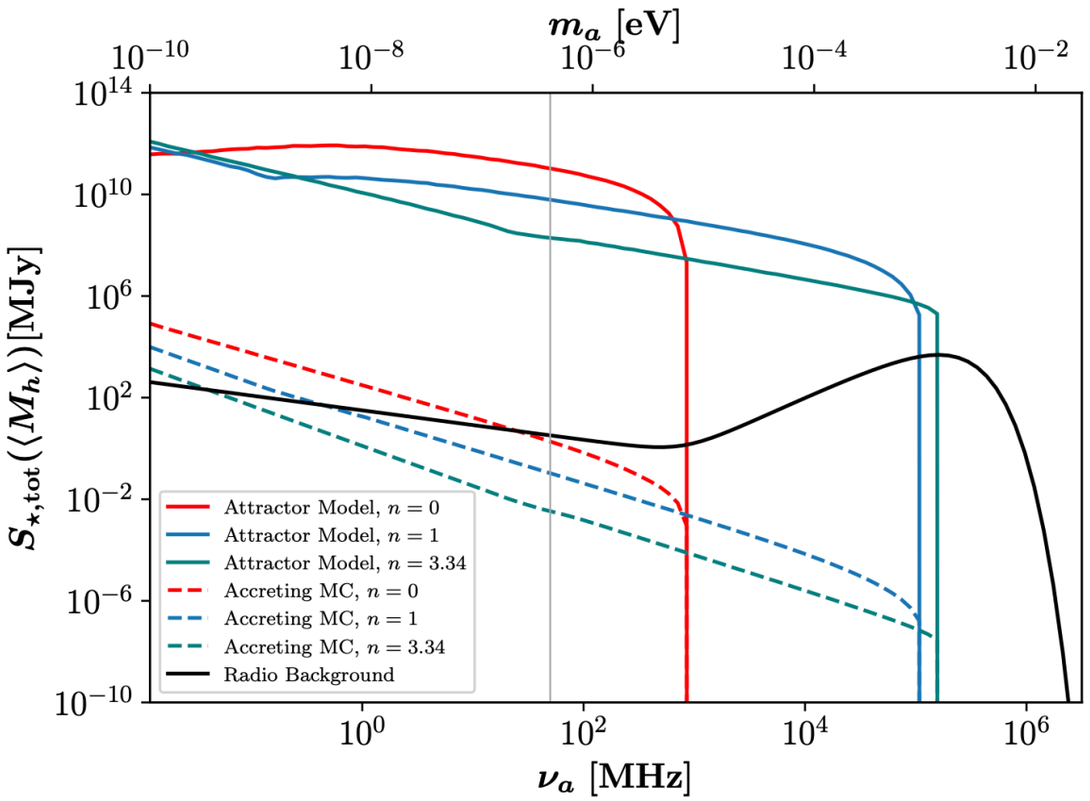

Figure 6: Total predicted radio flux $S_{*,tot}(m_a, n)$ from photon-critical axion stars with the general accretion rate (23) by Levkov in solid lines and with the accretion rate in eq. (38) in dashed lines, for $g_{a\gamma\gamma} = 10^{-11}$ /GeV. Colored lines indicate the spectral line peak frequency at ν_a with temperature dependence n, black denotes the (continuous) radio backgrounds. The values taken here are $d_{\mathrm{obs}} = 50\,\mathrm{kpc}$.

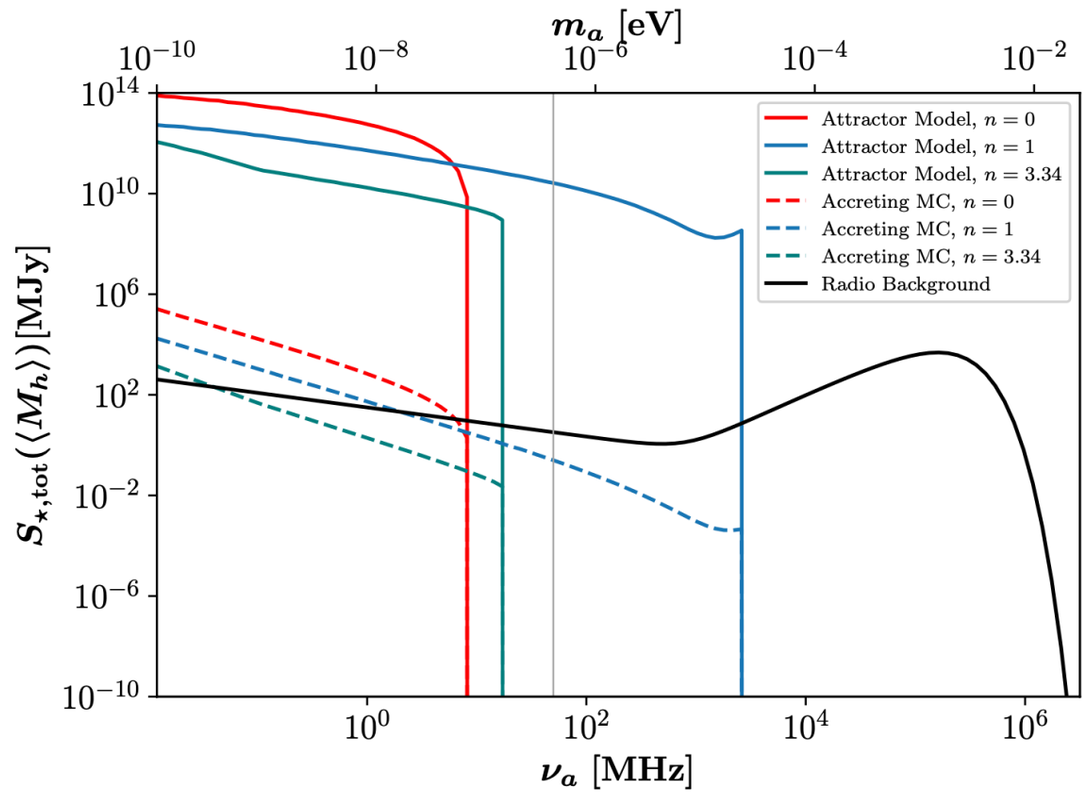

Figure 7: Total predicted radio flux $S_{*,tot}(m_a, n)$ from photon-critical axion stars with the general accretion rate (23) by Levkov in solid lines and with the accretion rate in eq. (38) in dashed lines, for $g_{a\gamma\gamma} = 10^{-12}$ /GeV. Colored lines indicate the spectral line peak frequency at ν_a with temperature dependence n, black denotes the (continuous) radio backgrounds. The values taken here are $d_{\mathrm{obs}} = 50\,\mathrm{kpc}$.

note: plotted are line fluxes from the Galaxy: everything above the measured (black solid) fluxes is basically ruled out

accretion rate based on core-halo relation versus maximal case $\delta M_* = \delta M_h$

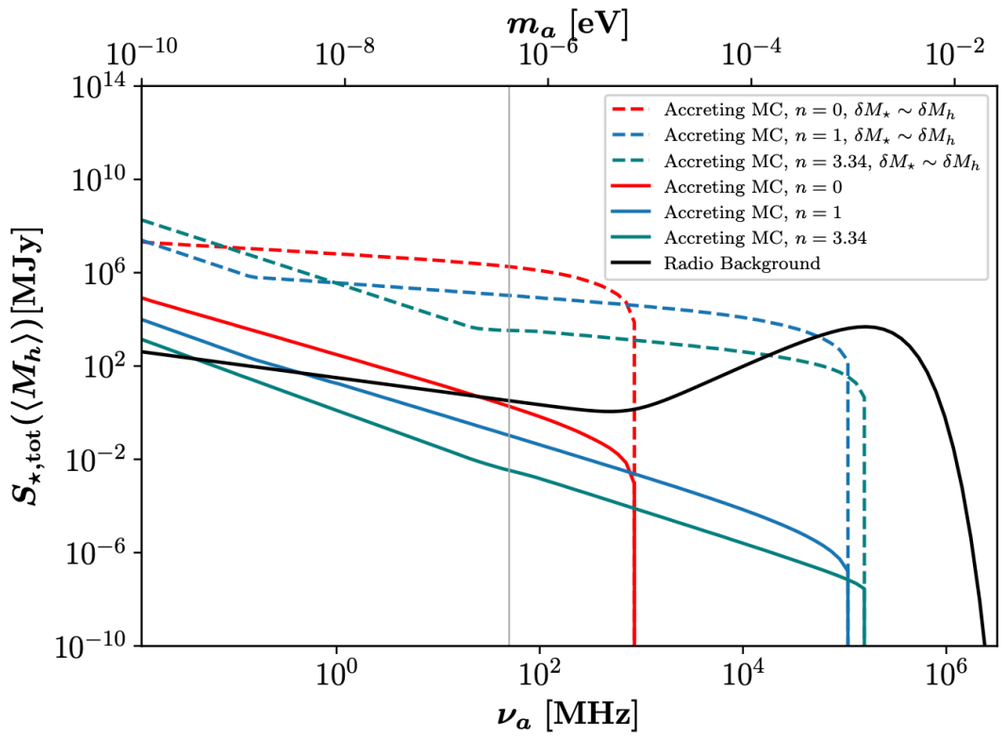

Figure 8: Total predicted radio flux $S_{*,tot}(m_a, n)$ from photon-critical axion stars with the accretion rate in eq. (38) in solid lines. The dashed lines show the same accretion scenario but without the surpression factor $\left(\frac{M_h}{M_{0,min}}\right)^{-2/3}$, i.e. for the most optimistic case of secondary accretion with $\delta M_\star = \delta M_h$. Colored lines indicate the spectral line peak frequency at ν_a with temperature dependence n, black denotes the (continuous) radio backgrounds. The values taken here are $d_{\mathrm{obs}} = 50\,\mathrm{kpc}$ and $g_{a\gamma\gamma} = 10^{-11}\,/\mathrm{GeV}$.

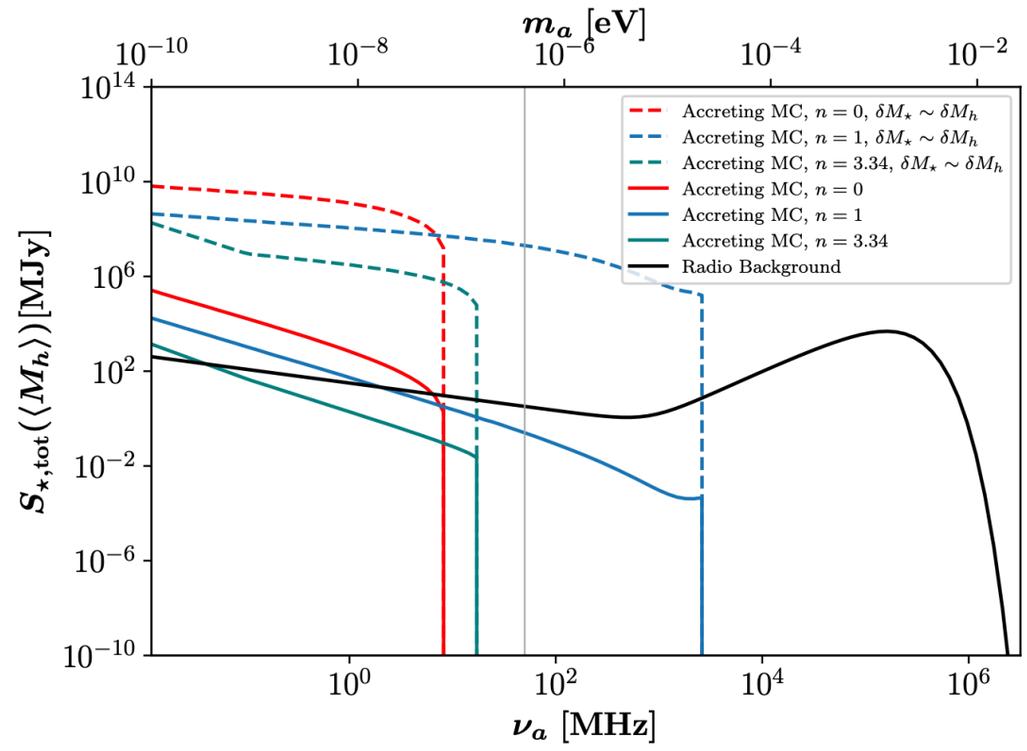

Figure 9: Total predicted radio flux $S_{*,tot}(m_a, n)$ from photon-critical axion stars with the accretion rate in eq. (38) in solid lines. The dashed lines show the same accretion scenario but without the surpression factor $\left(\frac{M_h}{M_{0,min}}\right)^{-2/3}$, i.e. for the most optimistic case of secondary accretion with $\delta M_\star = \delta M_h$. Colored lines indicate the spectral line peak frequency at ν_a with temperature dependence n, black denotes the (continuous) radio backgrounds. The values taken here are $d_{\mathrm{obs}} = 50\,\mathrm{kpc}$ and $g_{a\gamma\gamma} = 10^{-12}\,/\mathrm{GeV}$.

note: plotted are line fluxes from the Galaxy: everything above the measured (black solid) fluxes is basically ruled out

Conclusions 1

1.) Linelike radio emissions from dark matter-ALP conversion into photons in magnetic fields may be detectable with current and future radio telescopes such as LOFAR and SKA

2.) However, the most crucial (and least known) parameter is the magnetic field power on the ALP mass scale which is in the meter regime for μeV ALP masses and strongly suppresses the signal

3.) Resonant conversion around compact stellar objects may give interesting signals less dependent on magnetic field structure

Conclusions 2

4.) Spontaneous decay (interesting above ~10^{-5} eV) and parametric amplification in ALP stars are independent of magnetic fields, but the latter depends a lot on ALP star structure and their formation (not well understood yet but interesting conceptual questions)

5.) ALP accretion onto mini clusters and/or ALP stars can result in explosive conversion into radio photon lines of those ALP stars above a photon-coupling dependent critical mass; can lead to strong radio lines and thus constraints (so far Galactic signal considered)